Korean J. Chem. Eng., **27**(4), 1226-1232 (2010)
DOI: 10.1007/s11814-010-0184-9

Mixing parameters for an airlift bioreactor considering constant cross sectional area of riser to downcomer: Effect of sparging gas location

Jamshid Behin† and Azade Ahmadi

Department of Chemical Engineering, Faculty of Engineering, Razi University, Kermanshah, Iran
(*Received 31 July 2009 • accepted 18 November 2009*)

Abstract−The effect of mode of sparging gas on the mixing parameters of an internal loop airlift bioreactor was investigated. Two bioreactors of identical volume of 14×10^3 cm^3 and the optimum riser to downcomer cross sectional area ratio of 0.6 were studied. In one bioreactor a gas sparger was located in the draft tube and in the annulus in another. Liquid mixing characteristics, i.e., mixing time and circulation time, were employed to describe the performance of the bioreactors. The tracer injection method was used to determine the mixing parameters. A mathematical modeling based on the tanks-in-series model was employed to characterize the hydrodynamics behavior of the bioreactors. Matlab 7.1 software was used to solve the model equations in the Laplace domain and determine the model parameter, the number of stages. A comparison between the simulation results and experimental data showed that the applied model can accurately describe the behavior of the bioreactors. The results showed that when the gas sparger was located in the draft tube, the liquid mixing time, circulation time, and the number of stage were less than while the gas sparger was located in annulus. This is due to more wall effects, more energy losses and pressure drop in the case of gas injection in the annulus.

Key words: Airlift Bioreactor, Circulation Time, Gas Sparger, Liquid Mixing Time, Mathematical Modeling, Tank-in-series Model

INTRODUCTION

Airlift bioreactors (ALRs) are a special type of multiphase, pneumatic contactors. Industrial applications of these bioreactors are in hydrogenation, oxidation, epoxidation, fermentation, production of single cell protein, cultivation of microorganisms and wastewater treatment in chemical and biochemical processes [1-6]. Airlift bioreactors have attracted considerable attention due to their simple mechanical design with no moving part, high capacity, good mixing, low cost, low shear stress and low power input [7-9].

The important hydrodynamic parameters of the airlift bioreactors are the liquid mixing time and the liquid circulation time (or liquid circulation velocity). These parameters are sensitive to superficial gas velocity and physical properties of the fluids, gas flow rate and bioreactor geometry and have been extensively studied because of their influence on mass transfer phenomena [10]. Muthukumar et al. [7], Freitas et al. [11] and Fadavi et al. [12] investigated the hydrodynamic behavior of concentric draft-tube type airlift bioreactors. They demonstrated that an increase in the air-flow rate decreases mixing and circulation times. Bando et al. [13] have studied the effect of mode of sparging gas on the liquid mixing time and derived an equation for the liquid mixing time. The liquid mixing time was reported shorter in the mode of sparging gas into the draft tube than in the mode of sparging gas into the annulus when the equipment is the same. Pollard et al. [14] have made comparisons between two ring sparger locations, draft tube and annulus, in a concentric pilot scale airlift bioreactor. The hydrodynamic performance of the bioreactor was improved by using a draft tube ring sparger rather than the annulus ring sparger. This was due to the influence of the ratio of the cross sectional area of the riser and downcomer (A_r/A_d) in conjunction with the effect of liquid velocity. In the studies of Muthukumar et al. [7], Bando et al. [13], Koide et al. [15] and Weiland [16], independently of the column diameter and mode of sparging gas, the liquid mixing time has a minimum when the diameter ratio is between 0.5 and 0.6, i.e., A_r/A_d: 0.33-0.56.

The residence time distribution (RTD) of a chemical reactor is a characteristic of the flow pattern that occurs in the reactor, being one of the most informative characterizations of the reactor. In actual operation, most airlift bioreactors lie somewhere between two extremes: plug flow and perfectly mixed flow. Deviation from the two ideal patterns can be caused by channeling of fluid, by recycling of fluid or by creation of stagnant regions in the vessel. The specific sections of the airlift bioreactors (riser, downcomer, gas-separator and bottom zones) are different hydrodynamically. When analyzing non-ideal reactors, the RTD alone is not sufficient to determine its performance and more information is needed. To understand RTD quantitatively the experimental data have to be fitted to an adequate model (the axial dispersion model or the tanks-in-series model) to describe non ideal reactor flow pattern [17,18]. The mixing model used in most of the previous investigations dealing with airlift bioreactors is an axial dispersion model. It should be noted that the axial dispersion model could describe satisfactorily only mixing, which slightly deviates from the plug flow. A tanks-in-series model used in this work is applicable to the whole mixing extent including perfect mixing and plug flow mixing. Moreover, the tanks-in-series model provides a set of first order differential equations that can be solved by using rather simple numerical techniques [19]. Prokop et

†To whom correspondence should be addressed.
E-mail: Behin@razi.ac.ir

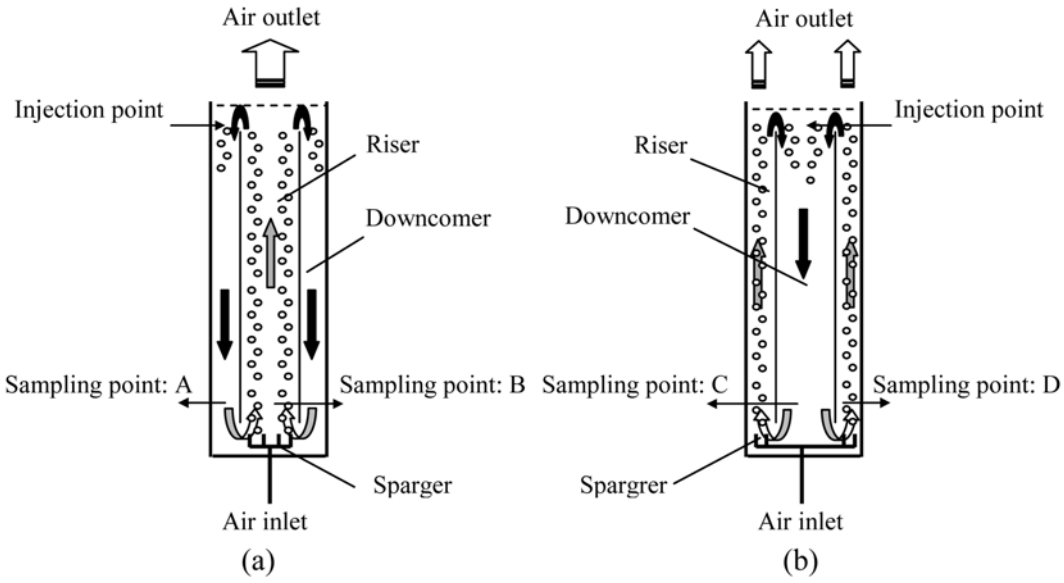

Fig. 1. Schematic of flow path in the internal loop airlift bioreactor (a) Sparger in draft tube (b) Sparger in annulus.

al. [20] and Erickson et al. [21] examined the performance of a multistage tower fermentor using a tanks-in-series model with back flow and achieved good results. Turner and Mills [22] pointed out that the tanks-in-series model is more realistic and advantageous compared with the axial dispersion model. Kanai et al. [23] applied the tanks-in-series model with back flow to simulate the continuous cultures in airlift bioreactors and to discuss their steady state performance. The experimental data and the predicted results were in good agreement. Znad et al. [19] applied a tanks-in-series model for mathematical modeling of the unsteady state performance of a semi batch operation in an internal loop airlift bioreactor. The seven stages in the riser, the ten stages in the downcomer and the first and ninth stages represent the bottom and top sections, respectively, of the airlift bioreactor. The experimental data and the predicted results were in good agreement. Choi [24] developed a tanks-in-series model for simulation of unsteady-state oxygen transfer in an external airlift reactor. The simulation results showed a good agreement with experimental results. Varedi Kolaei et al. [25] investigated mathematical modeling of a microbial biomass production in a stirred tank bioreactor and in an external airlift bioreactor. A model based on a tanks-in-series model without back-flow has been used to simulate the production of single cell protein in the external airlift bioreactor under an unsteady condition. Matlab software was used to solve the equations of the tanks-in-series model. The number of stages of the tanks-in-series obtained equals 16. Sikula et al. [26] used a tank-in-series model for mathematical modeling of fermentation of gluconic acid in three laboratory internal loop airlift bioreactors of different scale. The results of the simulations and experiments were in good agreement.

Bibliographic surveys [13-16] showed that sparger location affects the liquid mixing performance of the contactor. In this work, the effect of gas sparging location on mixing behavior of the internal loop airlift bioreactor (IL-ALR) was investigated by tank-in-series model. The riser to downcomer cross sectional area ratio (A_r/A_d) was kept constant at the reported optimum value of 0.60 in both modes of gas sparging.

1. Model Development Based on N-tanks-in-series Approach

A schematic of the internal loop air lift bioreactors used in this work was shown in Fig. 1. The gas was injected at two locations: draft tube (Fig. 1(a)) and annulus (Fig. 1(b)).

In the tanks-in-series model, the liquid flow in the airlift bioreactor is considered as a flow through a series of equally sized and well-mixed stirred stages, wherein the number of stages is the parameter that describes non-ideal flow. The tanks-in-series model without backflow is shown schematically in Fig. 2. The mixing characteristics of the riser, downcomer, top and bottom sections in airlift bioreactors are different. N_r stages in the riser are numbered, N_d stages in the downcomer are numbered, and two stages represent the bottom and top sections of the airlift bioreactor. To develop a mathematical expression for unsteady-state material balances in different

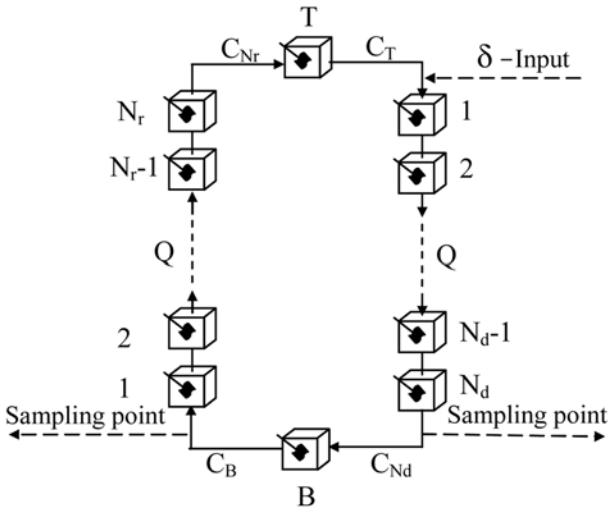

Fig. 2. Schematic diagram of the airlift bioreactor modeled by employing N-tanks-in-series approach.

sections of the bioreactor, the following assumptions were made to simplify this complex system:
- Chemical reactions are absent.
- Gas-liquid mass transfer is negligible.
- Flow is under isothermal conditions.
- The riser operates in the bubbly flow regime, i.e., low superficial gas velocity in the riser section.
- The flow in the riser and downcomer is all liquid.

The transfer function for the different sections of this model in the Laplace domain can be written as follows:

For the downcomer section:

$$\frac{\overline{C}_{N_d}}{\overline{C}_T} = \frac{1}{(\tau_d s+1)^{N_d}} \tag{1}$$

with

$$\tau_d = \frac{V_d/N_d}{Q} \tag{2}$$

For the bottom section:

$$\frac{\overline{C}_B}{\overline{C}_{N_d}} = \frac{1}{(\tau_B s+1)} \tag{3}$$

with

$$\tau_B = \frac{V_B}{Q} \tag{4}$$

For the riser section:

$$\frac{\overline{C}_{Nr}}{\overline{C}_B} = \frac{1}{(\tau_r s+1)^{Nr}} \tag{5}$$

with

$$\tau_r = \frac{V_r/N_r}{Q} \tag{6}$$

For the top section:

$$\frac{\overline{C}_T}{\overline{C}_{Nr}} = \frac{1}{(\tau_T s+1)^{Nr}} \tag{7}$$

with

$$\tau_T = \frac{V_T}{Q} \tag{8}$$

The inlet pulse was taken as a Dirac delta function, $\delta(t)$, since it had been determined that the injection process used in the experiments created pulses of sufficiently short duration compared to the total sampling time. The tracer signal after the m^{th} pass in the same point of injection, i.e., top of the downcomer, can be expressed as follows:

$$\frac{\overline{C}_{\delta,m}}{\overline{C}_{\delta,in}} = \frac{1}{(\tau_T s+1)^m (\tau_B s+1)^m (\tau_r s+1)^{mN_r} (\tau_d s+1)^{mN_d}} \tag{9}$$

The concentration of tracer in the bioreactor is the sum of all of the concentrations at the corresponding points, from the first, second, and succeeding passes. An analytical solution in the Laplace domain can be obtained for the mathematical model as follows:

$$\frac{\overline{C}_{\delta}}{\overline{C}_{\delta,in}} = \sum_{m=1}^{\infty} \frac{1}{(\tau_T s+1)^m (\tau_B s+1)^m (\tau_r s+1)^{mN_r} (\tau_d s+1)^{mN_d}} \tag{10}$$

This function was transformed back to the time domain by inverse Laplace transformation in Matlab 7.1. The calculated output function was then compared with the experimental output function to determine the stage numbers, which appear in the transfer function.

EXPERIMENTAL

Each bioreactor consists of a Plexiglas cylindrical column, 14 cm in internal diameter and 90 cm in height. A concentric draft tube 8.5 cm in internal diameter was inserted in one and 11 cm in internal diameter in another, as shown in Fig. 1. A vertical space of 5 cm was provided between the bottom of the column and the lower end of draft tube to allow liquid circulation. Tap water (17-20 °C) and air at ambient temperature (20 °C) and atmospheric pressure were used as the working fluids. The air flow rate was measured by a calibrated rotameter before entering the bioreactor. Air was sparged into the riser through 14 holes of 0.3 mm in diameter, arranged on a circle shape tube. Experiments were carried out in two bioreactors of identical geometrical structure. In one of them the gas sparger was located in the inner tube and in the annulus in another. The riser to downcomer cross sectional area ratio (A_r/A_d) was 0.60 in both modes of gas sparging. 50 ml of saturated solution of NaCl was injected (nearly ideal impulse) at the top of downcomer. The liquid was sampled at two different detection points located at 5 cm from the gas distributor in the riser and downcomer exits. Tracer concentrations were measured at equidistant time intervals, while the conductivity was analyzed by a conductivity-meter (Jenway; England). Before any data was collected, aeration of water was carried out over a long period of time to ensure that a steady flow distribution was established in the airlift bioreactor. To operate with complete gas disengagement, the bioreactor was always operated in the homogeneous bubble flow regimes, on the basis of visual observations. This regime occurs only at low superficial velocities of the input gas, when the induced liquid velocity is insufficient to entrain any gas bubbles into the downcomer [27]. The mixing parameters were determined directly from the tracer response curve. The liquid mixing time was defined as the time when the variation instantaneous tracer concentration became within ±5% of the constant value. The liquid circulation time, that is, the distance between adjacent tracer output peaks, was directly determined from the response curves. This is the necessary time for a liquid volume element to travel around the riser-downcomer circuit once.

RESULTS AND DISCUSSION

The obtained conductivity data was converted to concentration and recorded until the value became constant. The normalized dimensionless concentration of sodium chloride tracer, C, was calculated as follows:

$$C = \frac{C(t)-C(0)}{C(\infty)-C(0)} \tag{11}$$

To obtain more reliable values, all experiments were performed in duplicate with different gas flow rates of 13.2, 16.5, 20 $cm^3 \cdot s^{-1}$. The experimental data of the dimensionless tracer concentration are shown in Fig. 3 when the gas sparger was located in draft tube. The conductivity was measured in two sampling points of A (in downcomer)

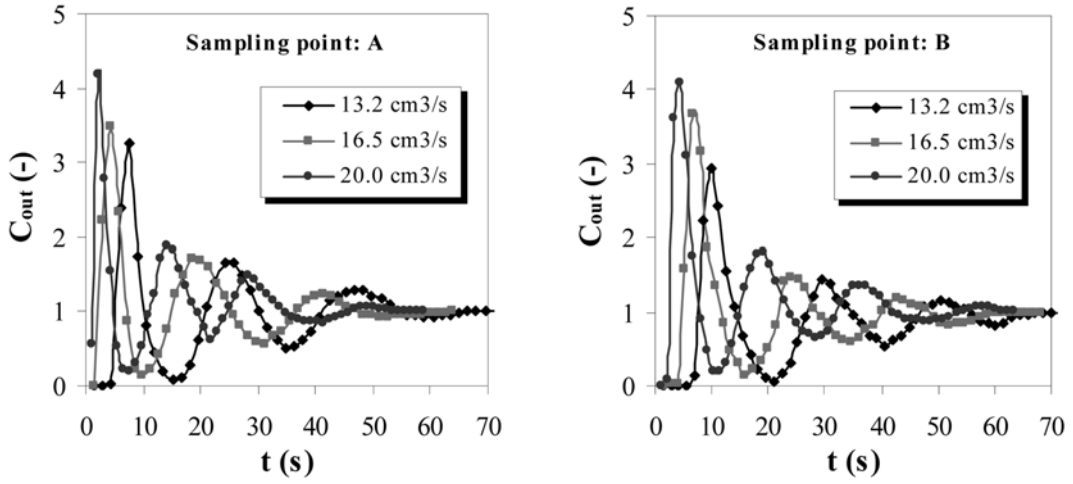

Fig. 3. Tracer responses at different gas flow rates (sparger in draft tube).

and B (in riser). The variance of the distribution curve decreases with increasing gas flow rate due to the high circulation velocity of the liquid. The curve tends to become narrow and long. The first peak appears early and the time interval between the first and the second peak is reduced. The first peaks characterize the residence time of liquid in the downcomer, while the differences between the first and second peaks characterize the residence time of liquid in the downcomer, riser, bottom and top sections.

Fig. 4 depicts the effect of gas flow rate on the dimensionless tracer concentration when the gas sparger was located in annulus. The conductivity was measured in two sampling points of C (in downcomer) and D (in riser). Compared to the mode of sparging gas in draft tube, the variance of distribution curves results in lower liquid circulation velocity and higher circulation time. The concentration of tracer varied smoothly after about three perfect peaks in all experiments.

The liquid mixing time (t_m) and circulation time (t_c) in both modes of sparging gas are presented in Table 1. These variables decrease with increasing gas flow rate. This is due to the increase in turbulence of the liquid with intense circulations, thus enhancing the mixing in the liquid phase. The variation was significant at higher gas flow rate because of higher driving force of liquid circulation gener-

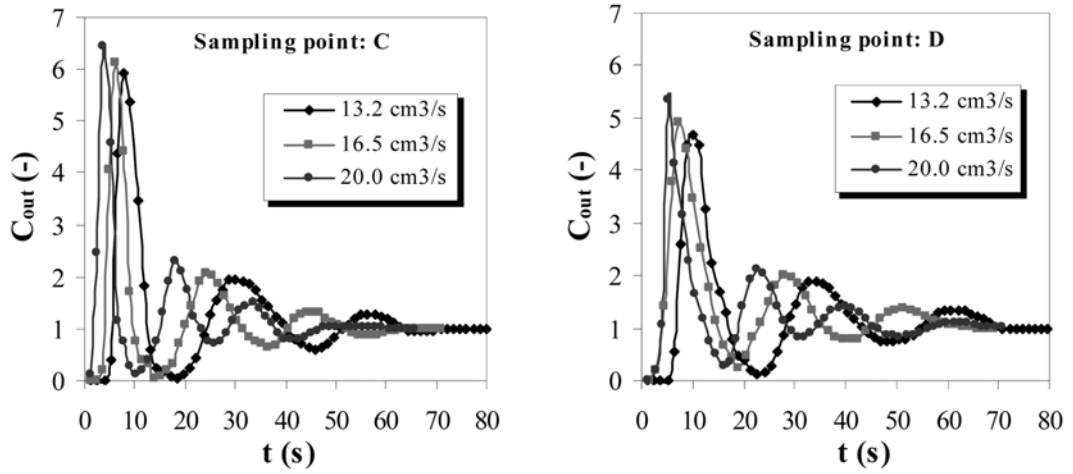

Fig. 4. Tracer responses at different gas flow rates (sparger in annulus).

Table 1. Mixing parameters in two modes of gas sparging

Gas flow rate ($cm^3 \cdot s^{-1}$)	Sparger in draft tube						Sparger in annulus					
	Sampling point: A			Sampling point: B			Sampling point: C			Sampling point: D		
	t_m	t_C	θ_m	t_m	t_C	θ_m	t_m	t_C	θ_m	t_m	t_C	θ_m
13.2	63.0	19.8	3.18	64.4	20.3	3.17	66.9	24.3	2.75	69.6	25.4	2.74
16.5	55.0	17.5	3.14	58.5	18.5	3.16	59.5	20.7	2.87	61.6	22.0	2.80
20.0	44.6	13.1	3.40	52.7	15.3	3.44	49.0	14.8	3.31	55.0	17.3	3.18

ated by higher gas hold-up. The mixing and circulation times were less, in general, when the gas sparger was in the draft tube. This condition becomes inverse in the case of gas sparging in the annulus. The pressure drop of two phase flow in the annulus was normally more than its corresponding value in the draft tube because of more friction loss on the two-cylindrical surface of the annulus than on internal surfaces of the draft tube. The hydraulic diameter of the annulus is less than its corresponding value for the draft tube. The friction loss of fluid in the two phase flow regime in the annulus becomes less than single phase flow and finally causes an increase in the liquid circulation velocity. Mixing in the airlift bioreactor is sometimes described in terms of a dimensionless mixing time, θ_m, defined as follows:

$$\theta_m = \frac{t_m}{t_C} \tag{12}$$

The dependence of dimensionless mixing time on gas flow rate is given in Table 1, in both modes of sparging gas. The dimensionless mixing time is nearly independent of the gas velocity, being only dependent on A_r/A_d.

1. Model Parameter Estimation

The relevant model parameter, that is, the number of stages, was determined by fitting the model prediction to experimental data through the popular least-squares technique in such a way as to give the best fit between experimental and theoretical data at the four gas flow

Table 2. Model parameters estimation at different gas flow rates

Sparger location	Q_g ($cm^3 \cdot s^{-1}$)	N_r	N_d	N_t
Draft tube	13.2	7.0	9.0	18.0
	16.5	5.5	7.0	14.5
	20.0	2.5	4.0	8.5
Annulus	13.2	8.5	9.5	20.0
	16.5	6.0	8.5	16.5
	20.0	3.0	5.0	10.0

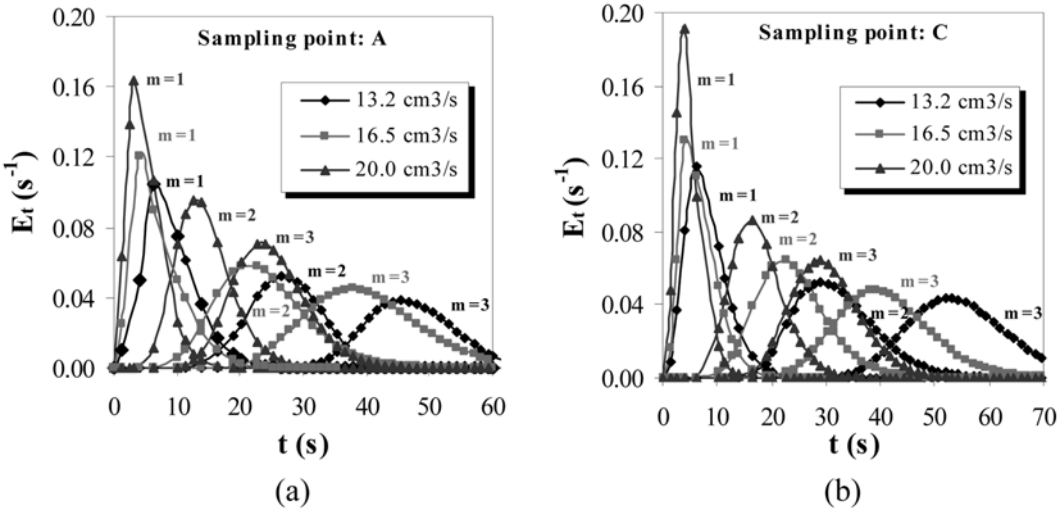

Fig. 5. The simulated RTD results of model for each pass (a) sparger in draft tube (b) sparger in annulus.

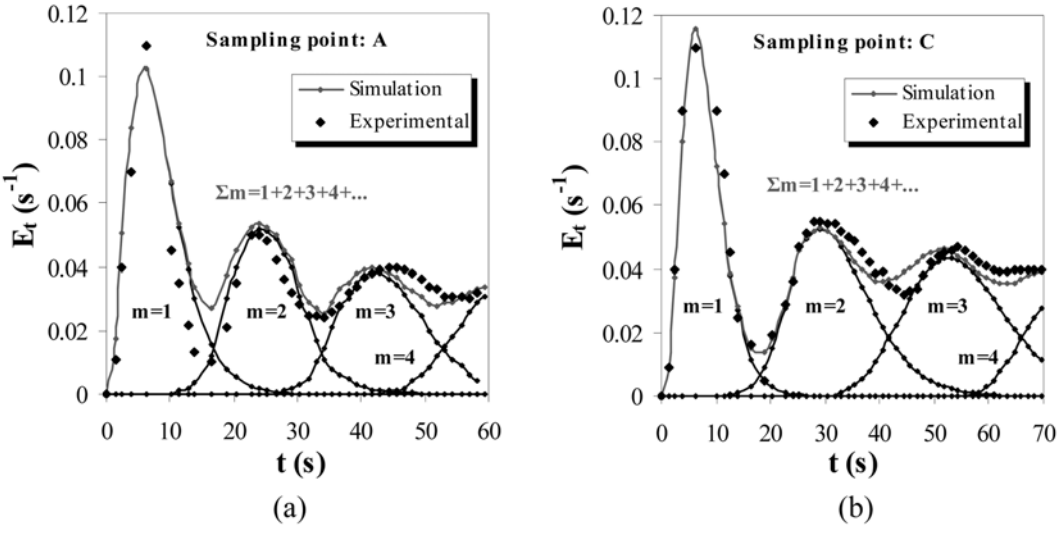

Fig. 6. The simulated RTD results of model for sum of passes and gas flow rate of 13.2 cm^3/s (a) sparger in draft tube (b) sparger in annulus.

rates. The number of stages was obtained by minimizing the residual sum of squares of the deviation between the experimental E-curve and that predicted by the model, i.e., the sum of squares error (SSE). This objective function was minimized by using the following expression:

$$SSE = \sum_{i}^{n} (C^{exp.}(t_i) - C^{mod.}(t_i))^2 \quad (13)$$

The model parameter, N_t, indicates the extent of longitudinal mixing in the bioreactor. The optimum values of the stage number are shown in Table 2. With increasing the superficial gas velocity, the total number of stages, N_t, decreases, and the flow regime moves towards mixed flow. The total number of stages varied from 20 to 10 with gas flow rate for sparging gas in the annulus. The corresponding values were 18 to 8.5 for sparging gas in the draft tube, which indicates a relatively higher intensity of mixing. This is due to the movement of gas bubbles forward that induce more turbulence of the fluid.

Figs. 5 and 6 show the simulation results of the N-tank-in-series model obtained by Matlab software in both modes of sparging gas. Considering the constant cross sectional area of riser to downcomer, the mixing was faster when the sparger was located in the draft tube than in the annulus.

CONCLUSIONS

The hydrodynamic mixing parameters of an internal loop airlift bioreactor of laboratory scale have been investigated by altering gas sparging position in inner and outer tube. A tanks-in-series model with a number-of-stages parameter was developed based on the Laplace transform. The study has led to the following conclusions:

- The good agreement obtained between the predicted and measured tracer concentrations demonstrates that the model can be used to simulate hydrodynamic behavior and RTD in an airlift loop bioreactor with satisfactory accuracy.

- With increasing gas flow rate (superficial gas velocity), the number of stages becomes less and liquid flow regime approaches to mixed flow pattern.

- In our experiment with riser to downcomer cross sectional area ratio of 0.6, the nearly complete and relatively fast mixing of liquid (fewer number of stages) could be achieved by inserting the gas sparger in the draft tube instead of the annulus. It is due to less wall effects, less pressure drop and energy losses.

NOMENCLATURE

A_d : cross-sectional area of the downcomer [cm^2]
A_r : cross-sectional area of the riser [cm^2]
$C(t)$: the instantaneous concentration of tracer [$mol \cdot cm^{-3}$]
$C(0)$: the initial concentration of tracer [$mol \cdot cm^{-3}$]
$C(\infty)$: the final concentration of tracer [$mol \cdot cm^{-3}$]
$\overline{C}_B$: the laplace transform of the tracer concentration from the bottom section [$mol \cdot cm^{-3}$]
$\overline{C}_T$: the laplace transform of the tracer concentration from the top section [$mol \cdot cm^{-3}$]
$\overline{C}_{N_d}$: the laplace transform of the tracer concentration from the N_d^{th} vessel [$mol \cdot cm^{-3}$]
$\overline{C}_{N_r}$: the laplace transform of the tracer concentration from the N_r^{th} vessel [$mol \cdot cm^{-3}$]
$C_{\delta,in}$: the laplace transform of the injection tracer concentration in the reactor [$mol \cdot cm^{-3}$]
$C^{exp.}$: the experimental RTD data [$mol \cdot cm^{-3}$]
$C^{mod.}$: the simulated model RTD response [$mol \cdot cm^{-3}$]
n : the number of experimental sample points [-]
N_d : the number of vessel in the downcomer section [-]
N_r : the number of vessel in the riser section [-]
N_t : total number of stage in the bioreactor [-]
Q : the liquid circulation flow rate [$cm^3 \cdot s^{-1}$]
t_m : the mixing time [s]
t_C : the circulation time [s]
U_L : the liquid circulation velocity [$cm \cdot s^{-1}$]
V_B : the volume of the bottom section [cm^3]
V_d : the volume of the downcomer [cm^3]
V_r : the volume of the riser section [cm^3]
V_T : the volume of the top section [cm^3]

Greek Letters

$\delta(t)$: Dirac delta function [-]
τ_B : the residence time of liquid in the bottom section [s]
τ_d : the residence time of liquid in each vessel of the downcomer [s]
τ_r : the residence time of liquid in each vessel of the riser [s]
τ_T : the residence time of liquid in the top section [s]

Subscripts

B : bottom
d : downcomer
r : riser
T : top
t : total

REFERENCES

1. B. Jajuee, A. Margaritis, D. Karamanev and M. A. Bergougnou, *Chem. Eng. J.*, **125**, 119 (2006).
2. P. Wang, M. Huang, T. K. Cheng, H. P. Chien and W. T. Wu, *J. Chem. Eng. Japan*, **35**, 354 (2002).
3. P. Zhang, M. Yang and X. Lu, *Chin. J. Chem. Eng.*, **15**, 196 (2007).
4. H. J. Song, H. Li, J. H. Seo, M. J. Kim and S. J. Kim, *Korean J. Chem. Eng.*, **26**, 141 (2009).
5. K. B. Lee, B. H. Chun, J. C. Lee, C. J. Park and S. H. Kim, *Korean J. Chem. Eng.*, **19**, 87 (2002).
6. D. J. Kim, D. H. Ahn and D. I. Lee, *Korean J. Chem. Eng.*, **22**, 85 (2005).
7. K. Muthukumar and M. Velan, *J. Chem. Eng. Japan*, **38**, 253 (2005).
8. T. J. Lin and P. Ch. Chen, *J. Chem. Eng.*, **40**, 69 (2005).
9. C. J. Park, *Korean J. Chem. Eng.*, **16**, 694 (1999).
10. T. Zhang, J. Wang, Z. Luo and Y. Jin, *J. Chem. Eng.*, **109**, 115 (2005).
11. C. Freitas and J. A. Teixeira, *Bioprocess. Eng.*, **18**, 267 (1998).
12. A. Fadavi and Y. Chisti, *Chem. Eng. J.*, **131**, 105 (2007).
13. Y. Bando, H. Hayakawa and M. Nishimura, *J. Chem. Eng. Japan*, **31**, 765 (1998).
14. D. J. Pollard, P. Ayazi Shamlou, M. D. Lilly and M. P. Ison, *Bioproc. Biosystems Eng. J.*, **15**, 279 (1996).

15. K. Koide, K. Horib, H. Kitaguchi and N. Suzuki, *J. Chem. Eng. Japan*, **17**, 547 (1984).
16. P. Weiland, *Ger. Chem. Eng.*, **7**, 374 (1984).
17. M. Gavrilescu and R. Z. Tudose, *Chem. Eng. Proc.*, **38**, 225 (1999).
18. O. Levenspiel, *Chem. React. Eng.*, 3rd Ed., John Wiley & Sons, New York, 295 (1999).
19. H. Znad, V. Báleš, J. Markoš and Y. Kawase, *Biochem. Eng. J.*, **21**, 73 (2004).
20. A. Prokop, L. E. Erickson, J. Fernandez and A. E. Humphrey, *Biotechnol. Bioeng.*, **11**, 945 (1969).
21. L. E. Erickson, S. S. Lee and L. T. Fan, *J. Appl. Chem. Biotechnol.*, **22**, 199 (1972).
22. J. R. Turner and P. L. Mills, *Chem. Eng. Sci*., **45**, 2317 (1990).
23. T. Kanai, T. Uzumaki and Y. Kawase, *Comput. Chem. Eng.*, **20**, 1089 (1996).
24. K. H. Choi, *Korean J. Chem. Eng.*, **16**, 441 (1999).
25. M. Varedi Kolaei, R. Karimzadeh, S. A. Shojaosadati and J. Towfighi, *Iranian. J. Biotechnol.*, **5**, 87 (2007).
26. I. Sikula, M. Jurašèík and J. Markoš, *Chem. Eng. Sci*., **62**, 5216 (2007).
27. M. Blažej, M. Kiša and J. Markos, *Chem. Eng. Proc.*, **43**, 1519 (2004).